International Journal of Solids and Structures 50 (2013) 2620–2630

Contents lists available at SciVerse ScienceDirect

International Journal of Solids and Structures

journal homepage: www.elsevier.com/locate/ijsolstr

Boussinesq problem with the surface effect and its application to contact mechanics at the nanoscale

Xiang Gao [a], Feng Hao [b], Daining Fang [a,*], Zhuping Huang [a,*]

[a] LTCS and Department of Mechanics and Engineering Science, College of Engineering, Peking University, Beijing 100871, China
[b] Department of Engineering Mechanics, Tsinghua University, Beijing 100084, China

ARTICLE INFO

Article history:
Received 5 January 2013
Received in revised form 31 March 2013
Available online 22 April 2013

Keywords:
Boussinesq problem
Surface effect
Contact mechanics
Size dependence
Scaling law

ABSTRACT

In the literature, it has been demonstrated that residual surface stress and surface elasticity are two equally important parts of surface stress theory and that, generally, neither of these aspects can be neglected. In this paper, we develop a non-classical formulation of the Boussinesq problem with the surface effect, in which both the residual surface stress and the surface elasticity are considered. To take into account the surface effect, a Lagrangian description of the governing equations of the surface is adopted. The theoretical and numerical results in this paper show that the contributions of the residual surface stress and the surface elasticity to the stresses and displacements at the surface are not always equal. The residual surface stress mostly influences the normal stress, whereas the surface elasticity is a dominant factor in the in-plane shear stress. As an application of this formulation, the three-dimensional Hertzian contact problem at the nanoscale is studied. It is concluded that the surface effect strengthens the elastic contact stiffness. The smaller the contact region, the larger the contact stiffness. Finally, in terms of the dimensionless surface parameters, the influences of the residual surface stress and the surface elasticity on the stresses and displacements are further studied, and a simple scaling law for the stresses and displacements at the surface is constructed for the first time.

1. Introduction

The Boussinesq problem has been a classical theme in the theory of elasticity and plays an important role in contact mechanics (Johnson, 1985). In recent years, microindentation and nanoindentation tests have become effective techniques for measuring the mechanical properties of materials (e.g., the elastic modulus and yield stresses of solids), including electromechanical intelligent materials and biomaterials with complex microstructures. For microindentation, the indentation depth ranges from hundreds of nanometers to 100 μm and experimental results (Feng and Nix, 2004; Ma and Clarke, 1995) show that a size effect arises with the indentation depth for the mechanical properties of materials. On the micron scale, the strain gradient continuum theory (Begley and Hutchinson, 1998; Huang et al., 2006; Nix and Gao, 1998) and the generalized continuum theory (Eringen, 1999) can be used to explain this size dependent phenomenon. However, when the indentation depth is in the nanometer range, the surface effect becomes prominent. Gerberich et al. (2002) noted that the surface to volume ratio should be an indispensable factor in nanoindentation, in which the indented materials are treated as elastic–plastic solids.

To explain the surface effect on the mechanical properties of materials, Gurtin and Murdoch (1975, 1978) systematically developed a surface stress theory. In their theory, a continuum description of the material surface was given, including the constitutive relations of the surface, which were based on Cauchy elasticity, and the conservation laws of the surface. With the rapid progress in nanoscience and nanotechnology, the Gurtin–Murdoch theory has been widely used and generalized to analyze the elastic properties of nanomaterials and nanostructures, such as nanowires (Chen et al., 2006; Jing et al., 2006; Park and Klein, 2008), nanofilms (Cammarata, 1994; Streitz et al., 1994a,b), composites with nano-inhomogeneities (Duan et al., 2005a; Sharma et al., 2003; Sharma and Wheeler, 2007) and nanoplates/shells (Altenbach and Eremeyev, 2011; Altenbach et al., 2012). Chen et al. (2006) and Jing et al. (2006) measured the effective flexural moduli of ZnO and silver nanowires, respectively, both of which were size dependent. The theoretical interpretations that are based on the surface effect are in good agreement with the experimental data. Park and Klein (2008) studied the surface stress effects on the resonant properties of metal nanowires, in which the importance of the residual surface stress was emphasized. Sharma and Ganti (2004) and Duan et al. (2005b) studied the eigenstrain problem

* Corresponding authors.
E-mail addresses: fangdn@pku.edu.cn (D. Fang), huangzp@pku.edu.cn (Z. Huang).

0020-7683/$ - see front matter © 2013 Elsevier Ltd. All rights reserved.
http://dx.doi.org/10.1016/j.ijsolstr.2013.04.007

for spherical nano-inhomogeneities with the interface effect and concluded that the Eshelby tensor is size dependent and position dependent in this case. Dingreville et al. (2005) suggested a framework to incorporate the surface free energy and derived the effective elastic modulus tensors of nanosized structural elements that took into account the surface effect. Duan et al. (2005a) studied the effective elastic constants of solids that contained spherical nano-inhomogeneities by considering the interface stress effect. Altenbach and Eremeyev (2011) derived the governing equation for nonlinear shells at the nanoscale by taking into account the surface stresses, and Altenbach et al. (2012) then studied the surface visco-elasticity effects on the effective properties of thin-walled nanostructures. Dingreville and Qu (2008) derived a new relation between the interfacial excess energy and the interfacial excess stress, which can account for both the in-plane and transverse deformations of the real material interface.

In recent years, several new directions have been explored in the surface effect. For example, the conventional surface stress theory is generalized to consider the surface roughness (Weissmuller and Duan, 2008; Wang et al., 2010; Mohammadi and Sharma, 2012; Mohammadi et al., 2013), the curvature dependence of the surface energy is considered to investigate its influences on nanostructures (Chhapadia et al., 2011) and surface effects have been found to alter the electromechanical coupling or piezoelectricity of nanostructures (Dai et al., 2011; Dai and Park, 2013). It is should be noted that new computational methods, which are based on atomistic simulation, molecular dynamics and first principle, are also developed to model the surface effects in most of the above-mentioned works.

In the study of elastic contact problems with the surface effect, there are two types of models in the existing literature. The first type only considers the residual surface stress; the surface elasticity is neglected. For instance, Wang and Feng (2007) studied the effect of the residual surface stress on the elastic half-space problem at the nanoscale. Long et al. (2012) studied the two-dimensional Hertzian contact problem by considering the effect of the residual surface stress. On the contrary, the second type only considers the surface elasticity, and the effect of the residual surface stress is neglected. Zhao and Rajapakse (2009) obtained analytical solutions for a surface-loaded isotropic elastic layer with surface effects that were based on the Gurtin–Murdoch theory. In their solutions, the residual surface stress does not affect the elastic field in the bulk material. Note that surface Green functions with the surface effect are basic functions in contact problems. He and Lim (2006) derived the surface Green functions for a soft elastic half-space with surface stress under the assumptions that the soft half-space is impressible and the surface has the same elastic properties as its interior. In their work, only the residual surface stress is considered. Koguchi (2008) formulated three-dimensional surface Green functions for an anisotropic half-domain using the Stroh formalism and considering the anisotropy of the material surface. However, his results have a rather complicated integral form. Chen and Zhang (2010) presented the analytical Green's function solutions for an isotropic elastic half-space that was subjected to anti-plane shear deformation. Actually, it can be shown that both the residual surface stress and the surface elasticity are important for the study of the surface effect and that, in general, neither of these effects can be neglected. Nevertheless, in most of the above-mentioned works, only one of these effects was considered. Therefore, nobody can answer the question of whether the contributions of the residual surface stress and of the surface elasticity to the stresses and displacements at the surface are equal or not.

In this paper, we focus on developing a non-classical formulation of the Boussinesq problem by considering both the residual surface stress and the surface elasticity. A Lagrangian description of the governing equations of the surface is adopted, and analytical solutions of the two-dimensional and three-dimensional Boussinesq problems with the surface effect are derived. These solutions can be used to clarify the influences of the residual surface stress and the surface elasticity on the elastic field in the bulk, and it is shown that their influences are not always equal. For some components of the stress/displacement, the influence of the residual surface stress is dominant, and, for other components of the stress/displacement, the influence of the surface elasticity can be pronounced. As an application of our developed theory, the three-dimensional Hertzian contact problem at the nanoscale is investigated, and its analytical solutions are obtained. For the first time, we suggest a simple scaling law for analyzing the contributions of the residual surface stress and the surface elasticity to the stresses and displacements at the surface. It should be mentioned that, for simplicity, the adhesion work (Johnson et al., 1971) and the adhesion force (Derjaguin et al., 1975) are not considered in the contact problem.

The present paper is organized as follows. A brief introduction to the fundamental equations of the surface that were developed by us is given in Section 2. The solutions of the Boussinesq problem with residual surface stress and surface elasticity are formulated in Section 3. For different types of distributed surface tractions, analytical solutions and their numerical results for half-plane problems are then presented in Section 4. As an example, a three-dimensional Hertzian contact problem at the nanoscale is investigated in Section 5. In Section 6, a simple scaling law for the stresses and displacements at the surface is suggested.

2. The fundamental equations of the surface

Atoms at the surface experience a different local environment than atoms in the bulk of materials, and the energy states and equilibrium positions of these atoms will generally differ from those of atoms in the interior. This difference is the physical origin of surface excess free energy and surface stress. For liquids, due to the atomic mobility, the number of surface atoms increases during stretching because the interior atoms in the liquid can freely flow to the surface, and, therefore, the surface stress is constant under stretching. While the atomic mobility is really low in solids, the total amount of surface atoms remains constant under elastic stretching, and, thus, the surface stress of solids usually exhibits elastic properties.

In the surface stress theory of solids, the material surface is approximately regarded as a two-dimensional curved elastic surface that has no thickness. Even without an external load, there exists a nonzero residual surface stress, which will induce a residual elastic field in the bulk. Choosing the initial configuration (undeformed configuration) as the reference configuration, we adopt a Lagrangian description of the surface constitutive relations, in which the first Piola–Kirchhoff surface stress is used:

$$\boldsymbol{S}_s^{(in)} = \gamma_0^* \boldsymbol{i}_0 + (\gamma_0^* + \gamma_1^*)\mathrm{tr}(\boldsymbol{E}_s)\boldsymbol{i}_0 - \gamma_0^*(\nabla_{0s}\boldsymbol{u}) + \gamma_1 \boldsymbol{E}_s \tag{1}$$

$$\boldsymbol{S}_s^{(ou)} = \gamma_0^*(u^\lambda B_{\lambda\alpha} + u^n_{,\alpha})\boldsymbol{A}_3 \otimes \boldsymbol{A}^\alpha \tag{2}$$

where Eqs. (1) and (2) are the "in-plane" and "out-plane" terms of the first Piola–Kirchhoff surface stress, respectively. $\mathbf{i}_0$ is the two-dimensional unit surface tensor in the reference configuration. $\boldsymbol{B} = B_{\lambda\alpha}\boldsymbol{A}^\lambda \otimes \boldsymbol{A}^\alpha$ is the surface curvature tensor in the reference configuration. $\gamma_0^*, \gamma_1^*, \gamma_1$ are constants that reflect the intrinsic properties of the material surface, in which γ_0^* reflects the residual surface stress and γ_1^*, γ_1 reflect the elastic properties of the surface. The surface displacement $\boldsymbol{u}$ is decomposed into $\boldsymbol{u}_s = u^\alpha \boldsymbol{A}_\alpha$ in the tangent plane of the surface and into $\boldsymbol{u}_n = u^n \boldsymbol{A}_3$ along the normal of the surface in the reference configuration. In the infinitesimal deformation analysis, the surface strain $\boldsymbol{E}_s$ is defined as follows:

$$\boldsymbol{E}_s = \frac{1}{2}(\boldsymbol{u}\nabla_{0s} + \nabla_{0s}\boldsymbol{u}) \tag{3}$$

where ∇_{0s} denotes the surface gradient operator in the reference configuration. It should be noted that, when there is no surface deformation, i.e., $\boldsymbol{u} = \boldsymbol{0}$, we have

$$\boldsymbol{S}_s^{(in)} = \gamma_0^* \boldsymbol{i}_0, \quad \boldsymbol{S}_s^{(ou)} = 0 \tag{4}$$

which is just the well-known residual surface stress.

To solve the problems with the surface effect, another equation is needed to describe the equilibrium of the material surface, which is usually called the generalized Young–Laplace equation. From the stationary condition of a newly suggested energy functional, we derived a Lagrangian description of the Young–Laplace equation as follows:

$$\boldsymbol{A}_3 \cdot [\![\boldsymbol{S}^0]\!] \cdot \boldsymbol{A}_3 = -\boldsymbol{S}_{bis}^{(in)} : \boldsymbol{B} - \left(\boldsymbol{A}_3 \cdot \boldsymbol{S}_s^{(ou)}\right) \cdot \nabla_{0s} \tag{5}$$

$$\boldsymbol{P} \cdot [\![\boldsymbol{S}^0]\!] \cdot \boldsymbol{A}_3 = -\boldsymbol{S}_s^{(in)} \cdot \nabla_{0s} + \boldsymbol{B} \cdot \left(\boldsymbol{A}_3 \cdot \boldsymbol{S}_s^{(ou)}\right) \tag{6}$$

where $\boldsymbol{S}^0$ is the first Piola–Kirchhoff stress in the bulk and $[\![\boldsymbol{S}^0]\!]$ denotes the jump of the first Piola–Kirchhoff stress across the surface/interface. $\boldsymbol{P} = \boldsymbol{I} - \boldsymbol{A}_3 \otimes \boldsymbol{A}_3$ is the tangential projection operator, and $\boldsymbol{I}$ is the unit tensor in three-dimensional Euclidean space. For an initially planar surface, the curvature tensor $\boldsymbol{B}$ is zero. Here, we only consider infinitesimal deformations and give some basic equations of the surface/interface energy theory. For details, the reader may refer to the Refs. Huang and Wang (2006) and Huang and Sun (2007).

When the residual deformation that is induced by the surface/interface energy is small and the high-order small quantities in the expression of the strain $\tilde{\boldsymbol{\varepsilon}}$ relative to the stress-free configuration can be neglected, the strain and first Piola–Kirchhoff stress $\boldsymbol{S}^0$ in the bulk relative to the stress-free configuration can be approximately written as

$$\begin{aligned} \tilde{\boldsymbol{\varepsilon}} &= \boldsymbol{\varepsilon}^* + \boldsymbol{\varepsilon} \\ \boldsymbol{S}^0 &= \boldsymbol{\sigma}^* + \boldsymbol{\sigma} = \boldsymbol{\sigma}^* + \boldsymbol{L} : \boldsymbol{\varepsilon} \end{aligned} \tag{7}$$

where $\boldsymbol{\sigma}^*$ denotes the self-equilibrium residual stress in the bulk and $\boldsymbol{\varepsilon}^*$ is the corresponding residual strain. $\boldsymbol{\sigma}$ and $\boldsymbol{\varepsilon}$ denote the stress and strain in the bulk that are due to the an external load. $\boldsymbol{L}$ is the elastic stiffness tensor.

In the classical theory of elasticity, the equilibrium equation in the absence of a body force and Hooke's law for an isotropic elastic body are given as follows:

$$\begin{aligned} \boldsymbol{\sigma} \cdot \nabla &= 0 \\ \boldsymbol{\sigma} &= \lambda(tr\boldsymbol{\varepsilon})\boldsymbol{I} + 2\mu\boldsymbol{\varepsilon} \end{aligned} \tag{8}$$

where $\lambda = 2\mu v/(1-2v)$. μ and v are the shear modulus and the Poisson ratio, respectively. These equations, with the boundary conditions, constitute the complete equations that are needed to solve the problem with the surface effect. Many problems in classical elasticity and mesomechanics can be easily generalized to the nanoscale by considering the interface/surface effect, and it was shown that the obtained results are in good agreement with experimental data (Chen et al., 2006; Jing et al., 2006).

3. The formulation and solutions of the Boussinesq problem with the surface effect

Generally, the Boussinesq problem refers to when a concentrated force acts on the surface of an elastic half-space. Many contact problems are closely related to the Boussinesq problem. We now consider this problem with the surface effect using the surface stress theory. In this section, we mainly address two types of half-space problems: the plane case and the axisymmetric case. First, we list the general solutions of the half-space problem using the integral transformation method. Then, we discuss non-classical boundary conditions with the surface effect and finally derive analytical solutions of this type of boundary value problem.

3.1. General solutions of the Boussinesq problem

The general solutions of the stresses and displacements for the two-dimensional plane problem can be solved using Fourier integral transformations with respect to Cartesian coordinates (Fig. 1) (Selvadurai, 2000):

$$\begin{aligned} \sigma_z &= -\frac{1}{\sqrt{2\pi}} \int_{-\infty}^{+\infty} \xi^2 \overline{\phi} e^{-ix\xi} d\xi \\ \sigma_{xz} &= \frac{i}{\sqrt{2\pi}} \int_{-\infty}^{+\infty} \xi \frac{d\overline{\phi}}{dz} e^{-ix\xi} d\xi \\ \sigma_x &= \frac{1}{\sqrt{2\pi}} \int_{-\infty}^{+\infty} \frac{d^2\overline{\phi}}{dz^2} e^{-ix\xi} d\xi \end{aligned} \tag{9}$$

$$\begin{aligned} u_z &= \frac{1}{2\mu\sqrt{2\pi}} \int_{-\infty}^{+\infty} \left[(1-v)\frac{d^3\overline{\phi}}{dz^3} - (2-v)\xi^2 \frac{d\overline{\phi}}{dz}\right] \frac{e^{-ix\xi}}{\xi^2} d\xi \\ u_x &= \frac{i}{2\mu\sqrt{2\pi}} \int_{-\infty}^{+\infty} \left[(1-v)\frac{d^2\overline{\phi}}{dz^2} + v\xi^2\overline{\phi}\right] \frac{e^{-ix\xi}}{\xi} d\xi \end{aligned} \tag{10}$$

where $\overline{\phi}(\xi, z)$ is the Fourier transformation of the stress function and has the following form

$$\overline{\phi}(\xi, z) = (A + Bz)e^{-z|\xi|} \tag{11}$$

A and B are generally functions of the variable ξ and will be determined from the boundary conditions.

For the axisymmetric problem (Fig. 1), the stresses and displacements can be derived using Hankel transformations and can be expressed in terms of cylindrical coordinates (r, θ, z) (Selvadurai, 2000):

$$\begin{aligned} \sigma_z(r,z) &= \int_0^\infty \xi \left[(1-v)\frac{d^3\overline{\Phi}}{dz^3} - (2-v)\xi^2\frac{d\overline{\Phi}}{dz}\right] J_0(\xi r) d\xi \\ \sigma_{rz}(r,z) &= \int_0^\infty \xi^2 \left[v\frac{d^2\overline{\Phi}}{dz^2} + \xi^2(1-v)\overline{\Phi}\right] J_1(\xi r) d\xi \\ \sigma_r &= \int_0^\infty \xi \left[v\frac{d^3\overline{\Phi}}{dz^3} + (1-v)\xi^2\frac{d\overline{\Phi}}{dz}\right] J_0(\xi r) d\xi - \int_0^\infty \xi^2 \frac{1}{r}\frac{d\overline{\Phi}}{dz} J_1(\xi r) d\xi \\ \sigma_\theta &= \int_0^\infty \xi v \left(\frac{d^3\overline{\Phi}}{dz^3} - \xi^2\frac{d\overline{\Phi}}{dz}\right) J_0(\xi r) d\xi + \int_0^\infty \xi^2 \frac{1}{r}\frac{d\overline{\Phi}}{dz} J_1(\xi r) d\xi \end{aligned} \tag{12}$$

$$\begin{aligned} u_r(r,z) &= \frac{1}{2\mu}\int_0^\infty \xi^2 \frac{d\overline{\Phi}}{dz} J_1(\xi r) d\xi \\ u_z(r,z) &= \frac{1}{2\mu}\int_0^\infty \xi \left[(1-2v)\frac{d^2\overline{\Phi}}{dz^2} - 2(1-v)\xi^2\overline{\Phi}\right] J_0(\xi r) d\xi \end{aligned} \tag{13}$$

where $J_n(\xi r)$ denotes the nth Bessel function of the first kind and

$$\overline{\Phi}(\xi, z) = (A' + B'z)e^{-\xi z} \tag{14}$$

is the Hankel transformation of Love's strain function, in which A' and B' will be determined from the boundary conditions. The zero-order Hankel transformation is simply a two-dimensional Fourier transformation of a circularly symmetric function.

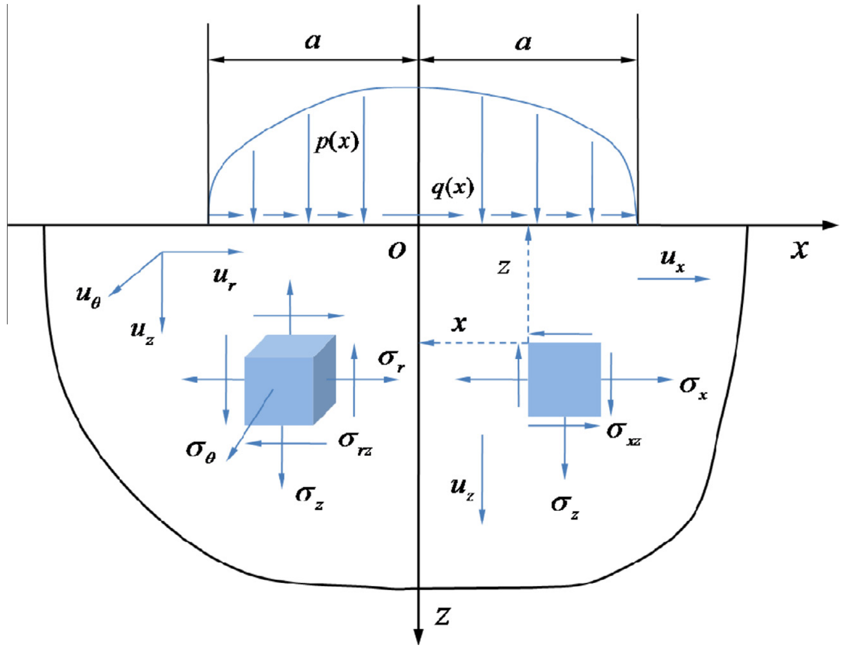

Fig. 1. A model of the Boussinesq problem.

3.2. Non-classical boundary conditions

This part is the core of the Boussinesq problem with the surface effect, in which the boundary conditions are different from those in the classical theory of elasticity. By applying the surface stress theory, we can write the non-classical boundary conditions Eqs. (5) and (6) as follows. For the plane problem, the surface boundary conditions are

$$\sigma_z|_{z=0} + p(x) = -\gamma_0^* \frac{\partial^2 u_z}{\partial x^2}, \quad \sigma_{xz}|_{z=0} + q(x) = -(\gamma_1^* + \gamma_1)\frac{\partial^2 u_x}{\partial x^2} \tag{15}$$

where u_x and u_z are the displacements along the x and z axes, respectively. p and q denote the distributed normal and tangential tractions, respectively.

For the axisymmetric problem, the boundary conditions are

$$\sigma_z|_{z=0} + p(r) = -\gamma_0^*\left(\frac{\partial^2 u_z}{\partial r^2} + \frac{1}{r}\frac{\partial u_z}{\partial r}\right), \quad \sigma_{rz}|_{z=0} + q(r) = -(\gamma_1^* + \gamma_1)\left(\frac{\partial^2 u_r}{\partial r^2} + \frac{1}{r}\frac{\partial u_r}{\partial r} - \frac{u_r}{r^2}\right) \tag{16}$$

where u_r and u_z are the radial and normal displacements, respectively. p and q denote the axisymmetric distributed normal and tangential tractions, respectively.

Because of the surface effect, the components of the stress across the surface do not equal the tractions that are applied by external loads. These non-classical mechanical boundary conditions reflect the influences of the surface energy, i.e., the residual surface stress γ_0^* leads to a normal discontinuity of the traction and the surface elasticity $\gamma_1^* + \gamma_1$ leads to a tangential discontinuity of the traction.

3.3. Analytical solutions of boundary-value problems

3.3.1. Plane problem

For the plane problem, we substitute the general solutions (9)–(11) into the boundary conditions (15) to obtain two equations with A and B,

$$-A\xi^2 + \overline{p}(\xi) = \frac{\gamma_0^*}{2\mu}[A|\xi| + (1-2\nu)B]\xi^2, \quad i(B - A|\xi|)\xi + \overline{q}(\xi) = \frac{(\gamma_1^* + \gamma_1)i}{2\mu}[A\xi^2 - 2(1-\nu)B|\xi|]\xi \tag{17}$$

where $\overline{p}(\xi)$ and $\overline{q}(\xi)$ are the Fourier transformations of the surface tractions,

$$\overline{p}(\xi) = \frac{1}{\sqrt{2\pi}}\int_{-\infty}^{+\infty} p(x)e^{ix\xi}dx, \quad \overline{q}(\xi) = \frac{1}{\sqrt{2\pi}}\int_{-\infty}^{+\infty} q(x)e^{ix\xi}dx \tag{18}$$

From Eqs. (17), we can solve A and B as follows:

$$A = \frac{-4 + 4(\nu-1)k|\xi|}{\eta(\xi)}\overline{p}(\xi) + \frac{2(2\nu-1)l\xi}{\eta(\xi)}\frac{\overline{q}(\xi)}{i}, \quad B = \frac{-2(k\xi^2 + 2|\xi|)}{\eta(\xi)}\overline{p}(\xi) + \frac{2\xi(l|\xi| + 2)}{\eta(\xi)}\frac{\overline{q}(\xi)}{i} \tag{19}$$

where $\eta(\xi) = \xi^2[-4 + 4(\nu-1)(k+l)|\xi| + (4\nu-3)kl\xi^2]$. It is worth noting that l and k are two intrinsic length scales that are related to the surface properties and are defined as

$$l = \frac{\gamma_0^*}{\mu}, \quad k = \frac{\gamma_1^* + \gamma_1}{\mu} \tag{20}$$

where l represents the residual surface stress and k represents the elastic properties of the material surface. Once A and B are determined, we can immediately write the solutions of the plane problem under normal pressure,

$$\begin{aligned}
\sigma_x &= -\sqrt{\frac{2}{\pi}}\int_0^{+\infty}\overline{p}(\xi)\frac{-4(k\nu\xi+1) + 2(k\xi^2+2\xi)z}{-4+4(\nu-1)(k+l)\xi+(4\nu-3)kl\xi^2}\cos(x\xi)e^{-z\xi}d\xi \\
\sigma_z &= -\sqrt{\frac{2}{\pi}}\int_0^{+\infty}\overline{p}(\xi)\frac{4[(\nu-1)k\xi-1] - 2(k\xi^2+2\xi)z}{-4+4(\nu-1)(k+l)\xi+(4\nu-3)kl\xi^2}\cos(x\xi)e^{-z\xi}d\xi \\
\sigma_{xz} &= -\sqrt{\frac{2}{\pi}}\int_0^{+\infty}\overline{p}(\xi)\frac{(4\nu-2)k\xi - 2(k\xi^2+2\xi)z}{-4+4(\nu-1)(k+l)\xi+(4\nu-3)kl\xi^2}\sin(x\xi)e^{-z\xi}d\xi
\end{aligned} \tag{21}$$

$$\begin{aligned}
u_x &= \frac{1}{\mu\sqrt{2\pi}}\int_0^{+\infty}\overline{p}(\xi)\frac{4(1-2\nu) - 2(k\xi^2+2\xi)z}{\xi[-4+4(\nu-1)(k+l)\xi+(4\nu-3)kl\xi^2]}\sin(x\xi)e^{-z\xi}d\xi + C_1 \\
u_z &= \frac{1}{\mu\sqrt{2\pi}}\int_0^{+\infty}\overline{p}(\xi)\frac{8(\nu-1) + 2(4\nu-3)k\xi - 2(k\xi^2+2\xi)z}{\xi[-4+4(\nu-1)(k+l)\xi+(4\nu-3)kl\xi^2]}\cos(x\xi)e^{-z\xi}d\xi + C_2
\end{aligned} \tag{22}$$

For P, which is the intensity of a concentrated normal force per unit length along the y-axis and acts on the surface at the origin, the Fourier transformation is $P/\sqrt{2\pi}$. By substituting this result into Eqs. (21) and (22), we can obtain the fundamental solutions of the two-dimensional Boussinesq problem.

If we set $l = k = 0$, these solutions will reduce to the classical solutions of the Boussinesq problem. For example, the results that were obtained by Wang and Feng (2007) are special cases if we neglect the surface elasticity and only set $k = 0$. The two integral constants C_1 and C_2 are fixed by datum that is chosen for the displacements. If we choose the tangential displacement to be zero at the origin and the normal displacement to vanish at $x = r_0 a$, we have $C_1 = 0$ and

$$u_z = \frac{1}{\mu\sqrt{2\pi}}\int_0^{+\infty}\overline{p}(\xi)\frac{8(\nu-1)+2(4\nu-3)k_r t}{t[-4+4(\nu-1)(k_r+l_r)t+(4\nu-3)k_r l_r t^2]} \times\left[\cos\left(\frac{x}{a}t\right)-\cos(r_0 t)\right]\mathrm{d}t \tag{23}$$

where $l_r = l/a$ and $k_r = k/a$ are two dimensionless parameters that reflect the surface effect.

When a concentrated tangential force acts on the half-plane, the stresses and displacements can be derived in a similar way that will not be reproduced here.

3.3.2. Axisymmetric problem

For the axisymmetric problem, the fundamental solutions of the Boussinesq problem can be derived in the same way. The substitution of the general solutions (12)–(14) into the boundary conditions (16) results in

$$\begin{aligned} &A'\xi^3\left(1+\frac{1}{2}l\xi\right)+B'\xi^2(1-2\nu)(1+l\xi) = -\overline{p}(\xi)\\ &A'\xi^3\left(1+\frac{1}{2}k\xi\right)-B'\xi^2\left(2\nu+\frac{1}{2}k\xi\right) = -\overline{q}(\xi)\end{aligned} \tag{24}$$

where $\overline{p}(\xi)$ and $\overline{q}(\xi)$ are the Hankel transformations of the axisymmetric surface tractions,

$$\overline{p}(\xi) = \int_0^\infty rp(r)J_0(\xi r)\mathrm{d}r, \quad \overline{q}(\xi) = \int_0^\infty rq(r)J_1(\xi r)\mathrm{d}r \tag{25}$$

We can then solve for A' and B', which can be expressed as

$$\begin{aligned} A' &= \frac{2(k\xi+4\nu)}{\xi^3 g(\xi)}\overline{p}+\frac{4(1-2\nu)(l\xi+1)}{\xi^3 g(\xi)}\overline{q},\\ B' &= \frac{2(k\xi+2)}{\xi^2 g(\xi)}\overline{p}+\frac{(-2)(l\xi+2)}{\xi^2 g(\xi)}\overline{q}\end{aligned} \tag{26}$$

where $g(\xi) = -4+4(\nu-1)(k+l)\xi+(4\nu-3)kl\xi^2$. The stresses and displacements under normal pressure are as follows:

$$\begin{aligned} \sigma_z &= \int_0^\infty \frac{\overline{p}}{g}\xi[4(1-\nu)k\xi+4+2(k\xi+2)\xi z]e^{-z\xi}J_0(\xi r)\mathrm{d}\xi\\ \sigma_{rz} &= \int_0^\infty \frac{\overline{p}}{g}\xi[2(1-2\nu)k\xi+2(k\xi+2)\xi z]e^{-z\xi}J_1(\xi r)\mathrm{d}\xi\\ \sigma_r &= \int_0^\infty \frac{\overline{p}}{g}\xi[4(k\nu\xi+1)-2(k\xi+2)\xi z]e^{-z\xi}J_0(\xi r)\mathrm{d}\xi+\frac{1}{r}\int_0^\infty\frac{\overline{p}}{g}[4(2\nu-1)\\ &\quad+2(k\xi+2)\xi z]e^{-z\xi}J_1(\xi r)\mathrm{d}\xi\\ \sigma_\theta &= \int_0^\infty \frac{\overline{p}}{g}\nu\xi^2(2k\xi+4)e^{-z\xi}J_0(\xi r)\mathrm{d}\xi-\frac{1}{r}\int_0^\infty\frac{\overline{p}}{g}[4(2\nu-1)\\ &\quad+2(k\xi+2)\xi z]e^{-z\xi}J_1(\xi r)\mathrm{d}\xi\end{aligned} \tag{27}$$

$$\begin{aligned} u_r &= \frac{1}{2\mu}\int_0^\infty\frac{\overline{p}}{g}[4(1-2\nu)-2(k\xi+2)\xi z]e^{-z\xi}J_1(\xi r)\mathrm{d}\xi\\ u_z &= \frac{1}{2\mu}\int_0^\infty\frac{\overline{p}}{g}[2(4\nu-3)k\xi+8(\nu-1)-2(k\xi+2)\xi z]e^{-z\xi}J_0(\xi r)\mathrm{d}\xi\end{aligned} \tag{28}$$

For P, the concentrated normal force that acts at the origin, the Hankel transformation is $P/(2\pi)$. By substituting this result into Eqs. (27) and (28), we can obtain the fundamental solutions of the three-dimensional Boussinesq problem. If we again set $l = k = 0$, these solutions will also reduce to the classical ones.

4. The elastic field in the half-plane and a numerical analysis

In this section, we use the plane problem as an example to investigate the surface effect on the stresses and displacements at the surface.

4.1. Analytical solutions of the distributed surface tractions

The solutions of the Boussinesq problem with the surface effect can be regarded as fundamental solutions to calculate the stresses and displacements of an elastic half-space that is subjected to distributed tractions with any form using the integral transformation method. In the two-dimensional plane problem, we consider the distributed normal pressure with the form (Johnson, 1985)

$$p = p_0(1-x^2/a^2)^n \tag{29}$$

acting on the strip $-a \le x \le a$. In the following, we consider some particular values of n in detail.

4.1.1. Uniform pressure ($n = 0$)

When $n = 0$, $p = p_0$ denotes a uniform pressure. The stresses and displacements at the surface ($z = 0$) can be written as

$$\begin{aligned} \overline{\sigma}_z &= -\frac{2p_0}{\pi}\int_0^{+\infty}\frac{4[k_r t(\nu-1)-1]}{-4+4(\nu-1)(k_r+l_r)t+(4\nu-3)k_r l_r t^2}\frac{\sin t}{t}\cos\left(\frac{x}{a}t\right)\mathrm{d}t\\ \overline{\sigma}_x &= -\frac{2p_0}{\pi}\int_0^{+\infty}\frac{-4(k_r\nu t+1)}{-4+4(\nu-1)(k_r+l_r)t+(4\nu-3)k_r l_r t^2}\frac{\sin t}{t}\cos\left(\frac{x}{a}t\right)\mathrm{d}t\\ \overline{\sigma}_{xz} &= -\frac{2p_0}{\pi}\int_0^{+\infty}\frac{(4\nu-2)k_r t}{-4+4(\nu-1)(k_r+l_r)t+(4\nu-3)k_r l_r t^2}\frac{\sin t}{t}\sin\left(\frac{x}{a}t\right)\mathrm{d}t\end{aligned} \tag{30}$$

$$\begin{aligned} \overline{u}_x &= \frac{p_0 a}{\mu\pi}\int_0^{+\infty}\frac{4(1-2\nu)}{-4+4(\nu-1)(k_r+l_r)t+(4\nu-3)k_r l_r t^2}\frac{\sin t}{t^2}\sin\left(\frac{x}{a}t\right)\mathrm{d}t\\ \overline{u}_z &= \frac{p_0 a}{\mu\pi}\int_0^{+\infty}\frac{2[4(\nu-1)+(4\nu-3)k_r t]}{-4+4(\nu-1)(k_r+l_r)t+(4\nu-3)k_r l_r t^2}\frac{\sin t}{t^2}\left[\cos\left(\frac{x}{a}t\right)-\cos(r_0 t)\right]\mathrm{d}t\end{aligned} \tag{31}$$

4.1.2. Hertz pressure ($n = 1/2$)

This value is the famous Hertz pressure, which is given by the Hertz theory and exerted between two frictionless elastic solids of revolution in the contact region; this pressure is expressed as

$$p = \frac{p_0}{a}\sqrt{a^2-x^2} \tag{32}$$

The stresses and displacements at the surface can be written as

$$\begin{aligned} \overline{\sigma}_z &= -p_0\int_0^{+\infty}\frac{4[(\nu-1)k_r t-1]}{-4+4(\nu-1)(k_r+l_r)t+(4\nu-3)k_r l_r t^2}\frac{J_1(t)}{t}\cos\left(\frac{x}{a}t\right)\mathrm{d}t\\ \overline{\sigma}_x &= -p_0\int_0^{+\infty}\frac{-4(k_r\nu t+1)}{-4+4(\nu-1)(k_r+l_r)t+(4\nu-3)k_r l_r t^2}\frac{J_1(t)}{t}\cos\left(\frac{x}{a}t\right)\mathrm{d}t\\ \overline{\sigma}_{xz} &= -p_0\int_0^{+\infty}\frac{(4\nu-2)k_r t}{-4+4(\nu-1)(k_r+l_r)t+(4\nu-3)k_r l_r t^2}\frac{J_1(t)}{t}\sin\left(\frac{x}{a}t\right)\mathrm{d}t\end{aligned} \tag{33}$$

$$\begin{aligned} \overline{u}_x &= \frac{p_0 a}{2\mu}\int_0^{+\infty}\frac{4(1-2\nu)}{-4+4(\nu-1)(k_r+l_r)t+(4\nu-3)k_r l_r t^2}\frac{J_1(t)}{t^2}\sin\left(\frac{x}{a}t\right)\mathrm{d}t\\ \overline{u}_z &= \frac{p_0 a}{2\mu}\int_0^{+\infty}\frac{8(\nu-1)+2(4\nu-3)k_r t}{-4+4(\nu-1)(k_r+l_r)t+(4\nu-3)k_r l_r t^2}\frac{J_1(t)}{t^2}\left[\cos\left(\frac{x}{a}t\right)-\cos(r_0 t)\right]\mathrm{d}t\end{aligned} \tag{34}$$

4.1.3. Uniform normal displacement ($n = -1/2$)

We shall show that a pressure distribution with the form

$$p = \frac{p_0 a}{\sqrt{a^2 - x^2}} \tag{35}$$

gives rise to a uniform normal displacement in the loaded strip for the classical case ($l_r = k_r = 0$). However, the surface effect will break this classical result, thus implying that u_z is not uniform in the loading zone. The stresses and displacements at the surface are

$$\begin{aligned} \overline{\sigma}_z &= -p_0 \int_0^{+\infty} \frac{4[(\nu-1)k_r t - 1]}{-4 + 4(\nu-1)(k_r + l_r)t + (4\nu-3)k_r l_r t^2} J_0(t) \cos\left(\frac{x}{a}t\right) dt \\ \overline{\sigma}_x &= -p_0 \int_0^{+\infty} \frac{-4(k_r \nu t + 1)}{-4 + 4(\nu-1)(k_r + l_r)t + (4\nu-3)k_r l_r t^2} J_0(t) \cos\left(\frac{x}{a}t\right) dt \\ \overline{\sigma}_{xz} &= -p_0 \int_0^{+\infty} \frac{(4\nu-2)k_r t}{-4 + 4(\nu-1)(k_r + l_r)t + (4\nu-3)k_r l_r t^2} J_0(t) \sin\left(\frac{x}{a}t\right) dt \end{aligned} \tag{36}$$

$$\begin{aligned} \overline{u}_x &= \frac{p_0 a}{2\mu} \int_0^{+\infty} \frac{4(1-2\nu)}{-4 + 4(\nu-1)(k_r + l_r)t + (4\nu-3)k_r l_r t^2} \frac{J_0(t)}{t} \sin\left(\frac{x}{a}t\right) dt \\ \overline{u}_z &= \frac{p_0 a}{2\mu} \int_0^{+\infty} \frac{8(\nu-1) + 2(4\nu-3)k_r t}{-4 + 4(\nu-1)(k_r + l_r)t + (4\nu-3)k_r l_r t^2} \frac{J_0(t)}{t} \left[\cos\left(\frac{x}{a}t\right) - \cos(r_0 t)\right] dt \end{aligned} \tag{37}$$

4.2. Numerical results and discussions

To investigate the surface effect on the elastic field, we mainly consider the two-dimensional plane problem in the subsequent numerical calculations. The numerical results are presented for metal aluminum (Al), which has a Poisson ratio of $\nu = 0.31$ and a shear modulus of $\mu = 26.56$ GPa. According to Medasani and Vasiliev (2009), the residual surface stress of metal Al is approximately $\gamma_0^* = 2.07N/m$. The surface elastic parameters are taken from Miller and Shenoy (2000) and from Sharma et al. (2003), i.e., $\gamma_1^* = 4.771$ N/m and $\gamma_1 = 1.319$ N/m for the Al surface. The two intrinsic length scales of the surface effect are thus $l = 0.078$ nm and $k = 0.2293$ nm. By substituting these material constants into the above analytical expressions, we can obtain the numerical results that are shown in the following figures. It should be noted that we plotted these figures by setting $a = 1$ nm and $r_0 = 5$.

As shown in Fig. 2, the distribution of the normal stress σ_z that is predicted by the classical theory experiences a singularity at the loading boundary and does not change smoothly; thus, this result appears unreasonable. The results that take into account the surface effect give a smooth distribution of the stress σ_z and overcome the singularity at the loading boundary $x = a$. The actual normal stress σ_z is smaller than the classical value in the loading zone and is larger outside of the zone. If the residual surface stress is ignored ($l_r = 0$), the values of σ_z reduce to the classical values; however, omitting the surface elasticity ($k_r = 0$) does not cause a significant change in σ_z, indicating that the residual surface stress is the dominant factor affecting the normal stress σ_z.

For the distributions of the stress σ_x at the surface, which are shown in Fig. 3, this stress has some similar properties to that in Fig. 2. The obvious difference is that the residual surface stress and the surface elasticity are equally important to σ_x so neglecting either of these effects would induce inaccurate results. The distributions of the shear stress σ_{xz} at the surface are presented in Fig. 4. As predicted by the classical theory of elasticity, the shear stress σ_{xz} at the surface is zero under any distributed normal tractions. This result does not hold if the surface effect is taken into account. The shear stress σ_{xz} becomes nonzero and has a maximum value at the loading boundary. It is also shown in analytical expressions (30), (33), and (36) that a nonzero distribution of σ_{xz} is totally attributed to the surface elasticity k_r. If the residual surface stress is ignored, the analytical expressions can give approximate results in the region that is far from the loading boundary.

The distributions of the surface displacements u_z and u_x are illustrated in Figs. 5 and 6. These two sets of figures both show that the surface deformations with the surface effects are smaller than

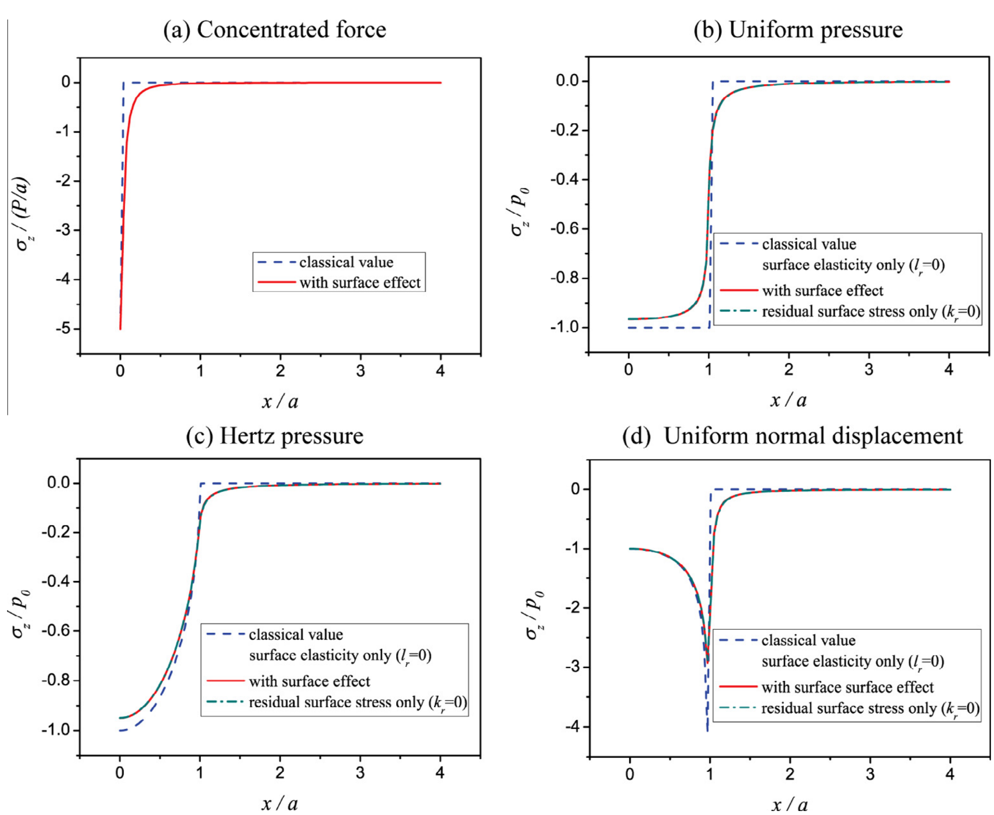

Fig. 2. The distributions of the normal stress σ_z at the surface.

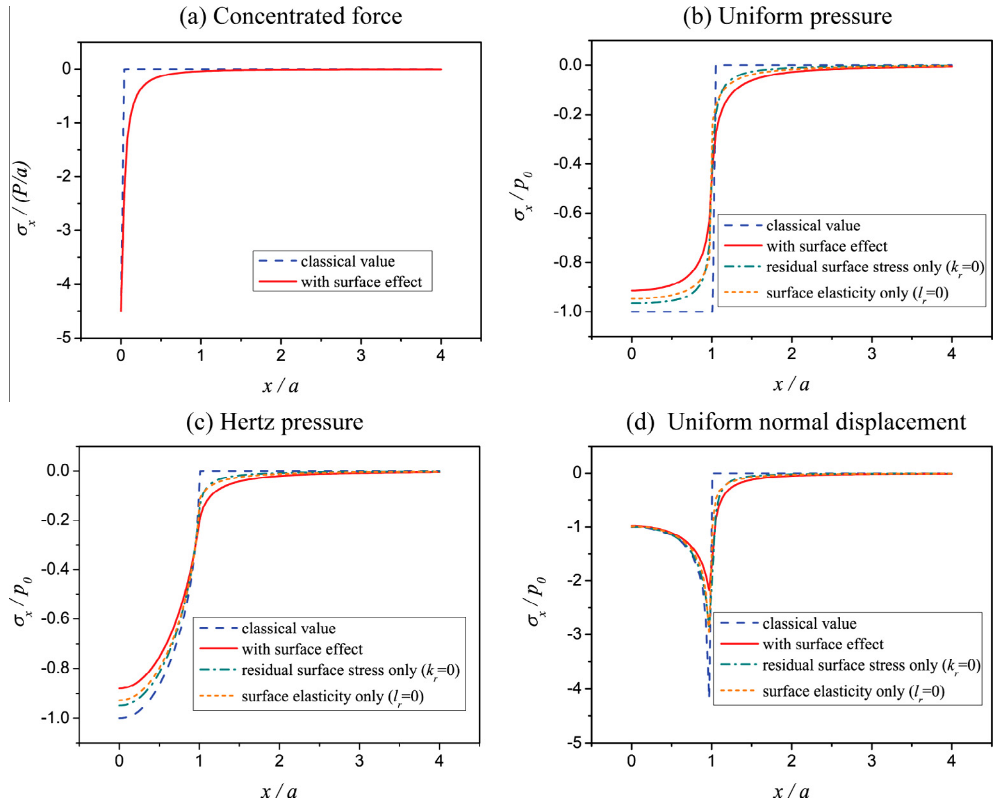

Fig. 3. The distributions of the normal stress σ_x at the surface.

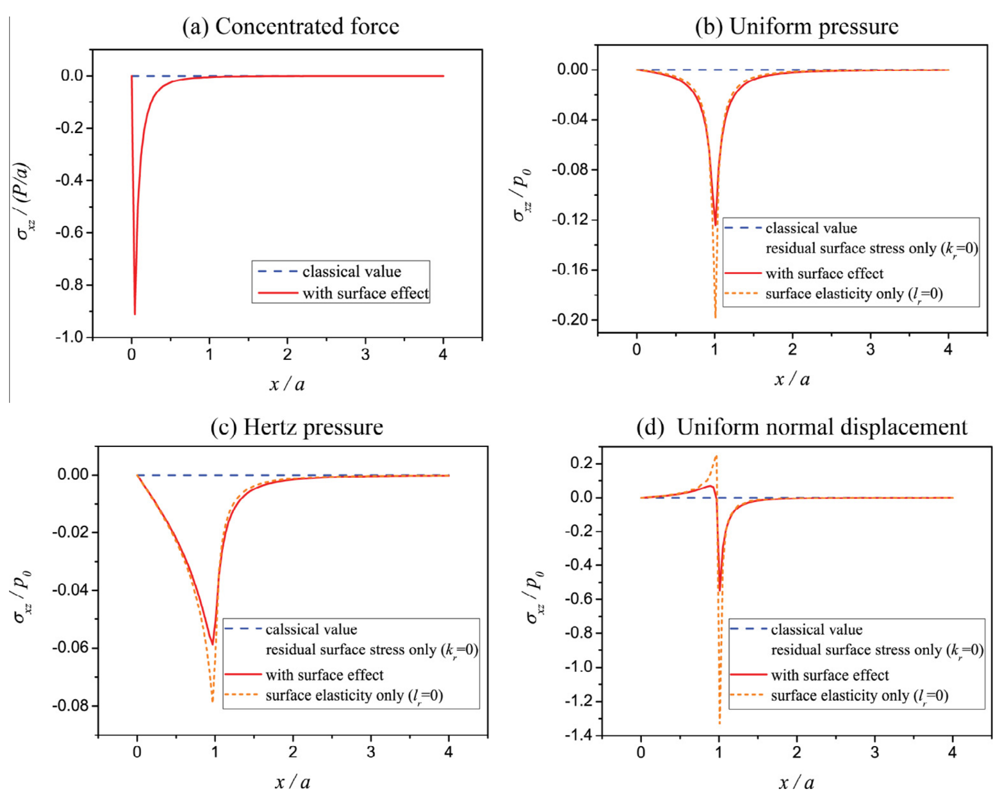

Fig. 4. The distributions of the shear stress σ_{xz} at the surface.

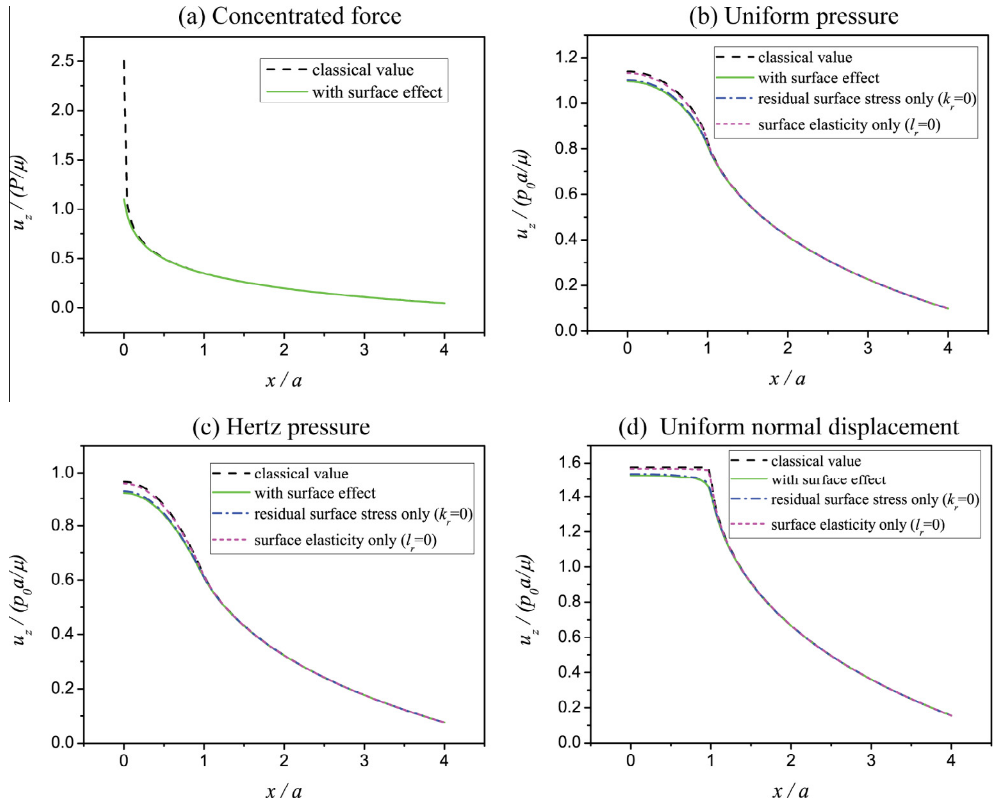

Fig. 5. The distributions of the surface normal displacement u_z.

those for the classical results, indicating that the surface effect strengthens the surface stiffness of materials. For the normal displacement u_z, it can be seen that the residual surface stress is dominant and that the surface elasticity is less important. An interesting phenomenon is illustrated in Fig. 5(d), i.e., the normal displacement becomes non-uniform at the nanoscale, which is quite different from the classical result. For the tangential displacement u_x, both the residual surface stress and the surface elasticity have appreciable influences on this displacement, so neither of these effects can be neglected. Additionally, the surface displacement gradients avoid discontinuities across the loading boundary when the surface effect is taken into account.

5. The Hertzian contact problem at the nanoscale

Experiments have shown that a size effect arises with indentation depth when the mechanical properties of materials are measured. However, the size effect in nanoindentation has not been well clarified. The surface effect may be an important factor in the study of nanoindentation. In this part we investigate the three-dimensional elastic contact problem with the surface effect. Assuming that a rigid spherical indenter with radius R is pressed into an elastic half-space, the interaction pressure in the contact region, according to the Hertz theory, has the form

$$p(r) = \frac{p_0}{a}\sqrt{a^2 - r^2} \quad (0 \le r \le a) \tag{38}$$

from which the total load is $P = \frac{2}{3}p_0\pi a^2$. In the Hertz contact model, the boundary condition for displacements within the contact region is

$$\bar{u}_z(r) \approx \delta - \frac{r^2}{2R} \tag{39}$$

where δ is the mutual approach of distant points in the two solids. $\bar{u}_z(r)$ is the surface normal displacement under the Hertz pressure that is calculated using Eq. (38) and is expressed as

$$\bar{u}_z(r) = \frac{p_0 a}{2\mu}\int_0^\infty \left[-\frac{\cos t}{t^2} + \frac{\sin t}{t^3}\right]\frac{2(4\nu-3)k_r t + 8(\nu-1)}{g(t;l_r,k_r)} J_0\left(\frac{r}{a}t\right)\mathrm{d}t \tag{40}$$

where $g(t;l_r,k_r) = -4 + 4(\nu-1)(k_r+l_r)t + (4\nu-3)k_r l_r t^2$. By taking the Taylor series expansion of Eq. (40) with respect to variable r, keeping up to the quadratic term and substituting this expansion into Eq. (39), we obtain

$$\delta = \frac{p_0 a}{2\mu}\int_0^\infty \left[-\frac{\cos t}{t^2} + \frac{\sin t}{t^3}\right]\frac{2(4\nu-3)k_r t + 8(\nu-1)}{g(t;l_r,k_r)}\mathrm{d}t \tag{41}$$

$$\frac{1}{2R} = \frac{p_0}{8\mu a}\int_0^\infty \left[-\cos t + \frac{\sin t}{t}\right]\frac{2(4\nu-3)k_r t + 8(\nu-1)}{g(t;l_r,k_r)}\mathrm{d}t \tag{42}$$

For $P = \frac{2}{3}p_0\pi a^2$, the above two equations result in

$$\delta = \frac{2}{R}a^2\frac{F(a)}{G(a)}, \quad PR = \frac{8\pi\mu a^3}{3}\frac{1}{G(a)} \tag{43}$$

where

$$\begin{aligned} F(a) &= \int_0^\infty \left[-\frac{\cos t}{t^2} + \frac{\sin t}{t^3}\right]\frac{2(4\nu-3)k_r t + 8(\nu-1)}{g(t;l_r,k_r)}\mathrm{d}t, \\ G(a) &= \int_0^\infty \left[-\cos t + \frac{\sin t}{t}\right]\frac{2(4\nu-3)k_r t + 8(\nu-1)}{g(t;l_r,k_r)}\mathrm{d}t \end{aligned} \tag{44}$$

are two functions of the radius a of the contact region and reflect the surface effect.

Generally, if the total load P and the radius of the indenter R are given, the mutual approach δ, the radius a of the contact region and the maximum pressure p_0 can be determined. Eq. (43) give new solutions of the normal frictionless contact of two elastic solids

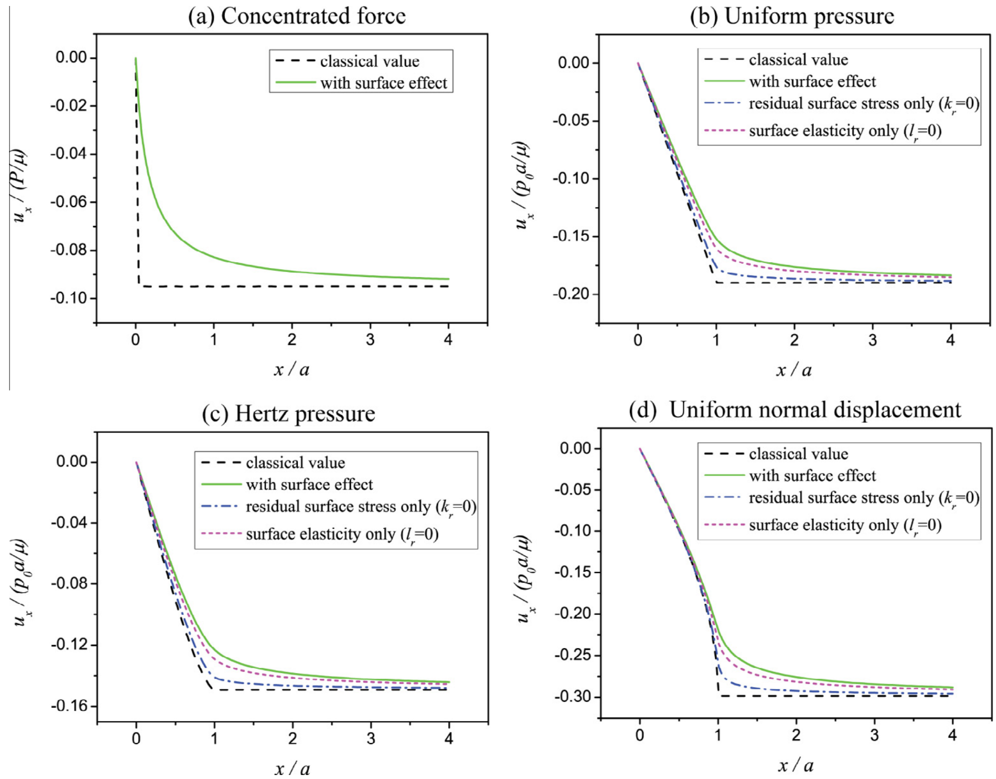

Fig. 6. The distributions of the surface tangential displacement u_x.

with the surface effect; however, these solutions are in implicit forms. When the two dimensionless surface parameters l_r and k_r are set to zero, i.e., the surface effect is neglected, the solutions in Eq. (43) will reduce to the classical results (Johnson, 1985).

To further elucidate the influence of the surface energy on the contact problem, we define the parameter $H = \mathrm{d}P/\mathrm{d}\delta$ to characterize the contact stiffness of elastic solids. We then obtain the dimensionless contact stiffness with the surface effect:

$$\frac{H}{H_0} = \frac{\pi(1-\nu)}{3} \cdot \frac{3G - aG'}{2FG + a(F'G - FG')} \tag{45}$$

where $H_0 = 4\mu a/(1-\nu)$ is the classical value of H without the surface effect. F' and G' denote the derivatives of functions F and G with respect to a. It is obvious that H/H_0 is size-dependent on a. Generally, the size of the contact region is related to the product PR, which is in Eq. (43).

Fig. 7 shows the size dependence of the contact stiffness H/H_0 that was defined above. The numerical results illustrate that, for metallic Al, the size effect becomes remarkable when $a < 10$ nm. At the nanoscale, the smaller the contact region, the larger the contact stiffness compared with the classical result. Additionally, we independently investigated the influences of the residual surface stress and the surface elasticity on the contact stiffness. It can also been seen from Fig. 7 that the residual surface stress is the main influence on the contact stiffness, compared with the surface elasticity and the combination of both factors results in a larger contact stiffness. Fig. 8 illustrates the relations between the mutual approach δ and the contact stiffness H/H_0 for different indenter sizes R. This figure demonstrates that an indenter with smaller size would experience a larger contact stiffness under the same mutual approach and that the contact stiffness increases as the mutual approach decreases. Generally, the material surface becomes stiffer due to the surface effect at the nanoscale.

6. A scaling law for the stresses and displacements at the surface

Surface/interface problems in nano- and microsystems are related to some characteristic length scales and dimensionless numbers (Zhao, 2012). It has been reported that many physical properties of nanostructured materials, such as the melting temperature and the elastic properties, become size dependent and obey a simple linear scaling law (Miller and Shenoy, 2000; Wang et al., 2006). These size dependent properties arise from the competition between surface/interface energies and energies that are stored in the bulk. By comparing the stresses and displacements at the surface for different distributed tractions, which are shown

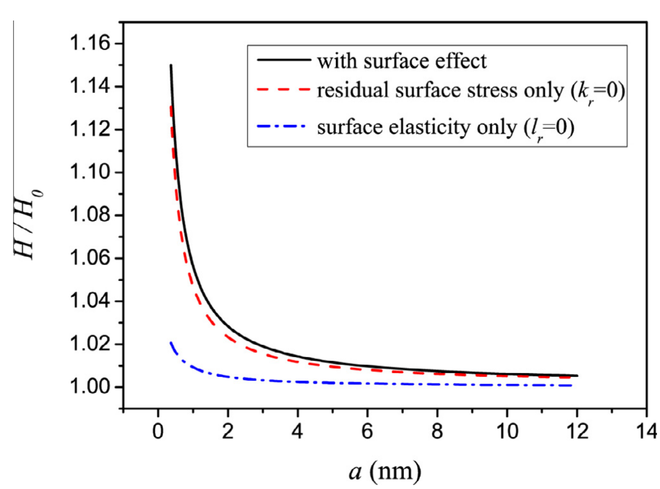

Fig. 7. The variations of the contact stiffness H/H_0 with the radius a of the contact region.

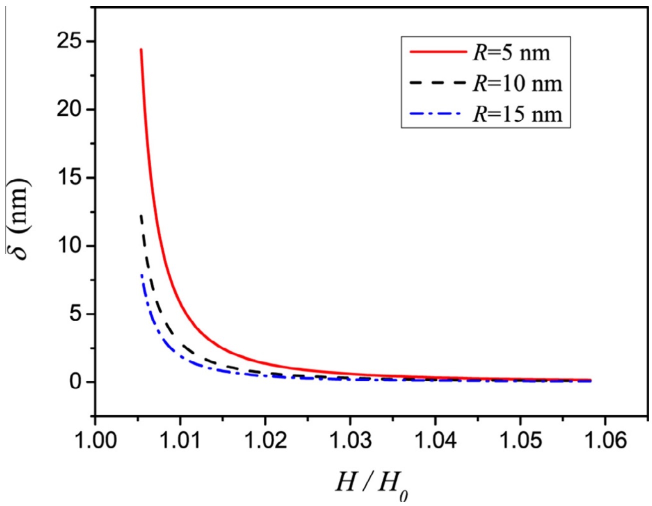

Fig. 8. The relation between the contact stiffness H/H_0 and the mutual approach δ.

in Section 4, with those of a concentrated normal force, we determine that the surface effect is characterized by the two surface constants l and k, which gives rise to two intrinsic length scales, $l = \gamma_0^*/\mu$ and $k = (\gamma_1^* + \gamma_1)/\mu$. For metals, these two intrinsic length scales are on the order of 0.01–1 nm. For polymers, these two intrinsic length scales are larger and can reach several or even a dozen nanometers because the shear modulus of polymers is much smaller than that of metals. Thus, the surface effect only becomes significant at the nanoscale.

In the two-dimensional plane problem, the surface energy affects the elastic fields at the surface via a function of the two dimensionless surface parameters l_r and k_r. For simplicity, we call this function the "surface correlation function". The surface correlation functions are listed in Table 1 for different stresses/displacements.

Notably, for a certain stress/displacement, the surface correlation functions are the same for different forms of the normal tractions that act on the surface. In Section 4, we treated the Boussinesq problem as fundamental solutions and found that the integral transformation procedure did not alter the surface correlation function. Generally, for a certain component of the stress/displacement, which is expressed as $T(x,a)$, its non-classical expression with the surface effect can be written as

$$T(x,a) = \int_0^{+\infty} \lambda(t,x,a) f(l_r, k_r, v, t) \mathrm{d}t \tag{46}$$

where $f(l_r, k_r, v, t)$ is the surface correlation function and $\lambda(t,x,a)$ denotes the remnant part of the integrand, which is relevant to the form of the surface traction. Then the classical result without the surface effect can then be obtained by setting $l_r = k_r = 0$.

According to the numerical calculation in Section 4, if the characteristic length of the contact problem (which is the radius a of the contact region in the present paper) is sufficiently large, then the two dimensionless surface parameters l_r and k_r are rather small compared with the number 1; thus, the product $l_r k_r$ is a high-order small quantity and may be neglected in the surface correlation function. Therefore, Eq. (46) can be approximately written as a simple linear scaling law as follows:

$$T(x,a) = T_0(x) + \frac{\widetilde{T}_1(x) l + \widetilde{T}_2(x) k}{a} = T_0(x) + \widetilde{T}_1(x) l_r + \widetilde{T}_2(x) k_r \tag{47}$$

where $T_0(x)$ represents the classical value and $\widetilde{T}_1(x), \widetilde{T}_2(x)$ are two position-dependent perturbation functions that represent the changes that arise from the surface effect. Generally, these functions can be expressed in the following form: $\widetilde{T}_i(x) = \int_0^{+\infty} \lambda(t,x,a) f_i(l_r, k_r, v, t) \mathrm{d}t$ $(i = 1, 2)$. For the stresses and displacements at the surface, their classical values can be easily calculated, and their perturbation functions are listed in Table 2.

Table 1
The surface correlation functions of the stresses and displacements.

Stress/ displacement	Non-classical case $f(l_r, k_r, v, t)$	Classical case $l_r = k_r = 0$
$\overline{\sigma}_z$	$\frac{4[(v-1)k_r t-1]}{-4+4(v-1)(k_r+l_r)t+(4v-3)k_r l_r t^2}$	1
$\overline{\sigma}_x$	$\frac{-4(k_r vt+1)}{-4+4(v-1)(k_r+l_r)t+(4v-3)k_r l_r t^2}$	1
$\overline{\sigma}_{xz}$	$\frac{(4v-2)k_r t}{-4+4(v-1)(k_r+l_r)t+(4v-3)k_r l_r t^2}$	0
$\overline{u}_x$	$\frac{4(1-2v)}{-4+4(v-1)(k_r+l_r)t+(4v-3)k_r l_r t^2}$	$2v - 1$
$\overline{u}_z$	$\frac{8(v-1)+2(4v-3)k_r t}{-4+4(v-1)(k_r+l_r)t+(4v-3)k_r l_r t^2}$	$2(1 - v)$

Table 2
The surface perturbation functions in the scaling law.

Stress/displacement	$f_1(l_r, k_r, v, t)$	$f_2(l_r, k_r, v, t)$
$\overline{\sigma}_z$	$\frac{-(v-1)t}{-1+(v-1)(k_r+l_r)t}$	0
$\overline{\sigma}_x$	$\frac{(1-v)t}{-1+(v-1)(k_r+l_r)t}$	$\frac{(1-2v)t}{-1+(v-1)(k_r+l_r)t}$
$\overline{\sigma}_{xz}$	0	$\frac{(2v-1)t}{-2+2(v-1)(k_r+l_r)t}$
$\overline{u}_x$	$\frac{-(2v-1)(v-1)t}{-1+(v-1)(k_r+l_r)t}$	$\frac{-(2v-1)(v-1)t}{-1+(v-1)(k_r+l_r)t}$
$\overline{u}_z$	$\frac{2(v-1)^2 t}{-1+(v-1)(k_r+l_r)t}$	$\frac{(2v-1)^2 t}{2[-1+(v-1)(k_r+l_r)t]}$

The linear scaling law in Eq. (47) elucidates the influences of the residual surface stress and the surface elasticity on a certain component of the stress/displacement. $\widetilde{T}_1(x) l_r$ represents the contribution of the residual surface stress, and $\widetilde{T}_2(x) k_r$ represents the contribution of the surface elasticity. From Table 2, it is apparent that the contribution of surface elasticity to σ_z is negligible and that the contribution of the residual surface stress to σ_{xz} is negligible, in good agreement with the numerical results. A numerical analysis can further confirm that this linear scaling law can give very accurate results for metal materials near the loading zone.

Similarly, it can be shown that the stresses and displacements at the surface of the three-dimensional Boussinesq problem have a similar scaling law; this derivation will not be reported here.

7. Conclusions

A non-classical formulation of the Boussinesq problem with the surface effect is presented in this paper. The following novel points can be concluded:

(1) In this formulation, the fundamental solutions for the concentrated forces that act on the boundary are derived, in which both the residual surface stress and the surface elasticity are taken into account. A series of theoretical and numerical results show that the influences of the residual surface stress and the surface elasticity on the stresses and displacements are not always equal. For instance, in a two-dimensional plane problem, the residual surface stress is the dominant factor that affects the stress component σ_z, whereas the surface elasticity is the dominant factor for the stress component σ_x.

(2) As an application of our formulation, we investigated the three-dimensional Hertzian contact problem at the nanoscale. Due to the surface effect, the elastic contact stiffness is size-dependent and is larger than the classical one. The smaller the size of the contact region, the larger the contact

stiffness. Additionally, the residual surface stress is the dominant factor that influences the contact stiffness. Moreover, it was found that, under a normal distributed traction, the elastic stress field is influenced by the material surface energy, which can be expressed in terms of the invariant "Surface Correlation Function". Based on this Surface Correlation Function, a scaling law for the stresses and displacements at the surface for the two-dimensional plane problem was suggested for the first time. Using this scaling law, the contributions of the residual surface stress and the surface elasticity can be quantitatively analyzed.

(3) The analysis that is presented in this paper indicates that a Lagrangian description of the basic equations of the surface/interface is preferred to correctly address the surface effect because the Lagrangian description of the surface/interface governing equations is based on a geometrically known reference configuration, which makes it more convenient to solve problems that are relevant to the surface/interface energy effect.

Note that in this paper, we concentrated on discussing the elastic property in the Hertzian contact problem with the surface effect; other relevant properties, such as the shape of the indenter, plastic deformation, adhesion force and adhesion work, are not considered. These properties may be important at the nanoscale and the work in the present paper lays the foundation for considering these factors in a future study.

Acknowledgements

The authors are grateful for the support from the National Natural Science Foundation of China under grants #11090330, #11090331 and #11072003. Support from the National Basic Research Program of China (#G2010CB832701) is also acknowledged. The authors extend their gratitude to the reviewers for their meaningful suggestions and the editors for their language editing service.

References

Altenbach, H., Eremeyev, V.A., 2011. On the shell theory on the nanoscale with surface stresses. Int. J. Eng. Sci. 49, 1294–1301.
Altenbach, H., Eremeyev, V.A., Morozov, N.F., 2012. Surface viscoelasticity and effective properties of thin-walled structures at the nanoscale. Int. J. Eng. Sci. 59, 83–89.
Begley, M.R., Hutchinson, J.W., 1998. The mechanics of size-dependent indentation. J. Mech. Phys. Solids 46, 2049–2068.
Cammarata, R.C., 1994. Surface and interface stress effects in thin films. Prog. Surf. Sci. 46, 1–38.
Chen, C.Q., Shi, Y., Zhang, Y.S., Zhu, J., Yan, Y.J., 2006. Size dependence of Young's modulus of ZnO nanowires. Phys. Rev. Lett. 96, 075505.
Chen, W.Q., Zhang, Ch., 2010. Anti-plane shear Green's functions for an isotropic elastic half-space with a material surface. Int. J. Solids Struct. 47, 1641–1650.
Chhapadia, P., Mohammadi, P., Sharma, P., 2011. Curvature-dependent surface energy and implications for nanostructures. J. Mech. Phys. Solids 59, 2103–2115.
Dai, S.X., Gharbi, M., Sharma, P., Park, H.S., 2011. Surface piezoelectricity: size effects in nanostructures and the emergence of piezoelectricity in non-piezoelectric materials. J. Appl. Phys. 110, 104305.
Dai, S.X., Park, H.S., 2013. Surface effects on the piezoelectricity of ZnO nanowires. J. Mech. phys. Solid 61, 385–397.
Derjaguin, B.V., Muller, V.M., Toporov, Y.P., 1975. Effect of contact deformations on the adhesion of particles. J. Colloid Interface Sci. 53, 316–326.
Dingreville, R., Qu, J., Cherkaoui, M., 2005. Surface free energy and its effect on the elastic behavior of nano-sized particles, wires and films. J. Mech. Phys. Solids 53, 1827–1854.
Duan, H.L., Wang, J., Huang, Z.P., Karihaloo, B.L., 2005a. Size-dependent effective elastic constants of solids containing nano-inhomogeneities with interface stress. J. Mech. Phys. Solids 53, 1574–1596.
Duan, H.L., Wang, J., Huang, Z.P., Karihaloo, B.L., 2005b. Eshelby formalism for nano-inhomogeneities. Proc. R. Soc. A 461, 3335–3353.
Dingreville, R., Qu, J., 2008. Interfacial excess energy, excess stress and excess strain in elastic solids: planar interfaces. J. Mech. Phys. Solids 56, 1944–1954.
Eringen, A.C., 1999. Microcontinuum field theories. Foundations and Solids, Vol. 1. Springer, New York.
Feng, G., Nix, W.D., 2004. Indentation size effect in MgO. Scr. Mater. 51, 599–603.
Gurtin, M.E., Murdoch, A.I., 1975. A continuum theory of elastic material surfaces. Arch. Ration. Mech. Anal. 57, 291–323.
Gurtin, M.E., Murdoch, A.I., 1978. Surface stress in solids. Int. J. Solids Struct. 14, 431–440.
Gerberich, W.W., Tymiak, N.I., Grunlan, J.C., Horstemeyer, M.F., Baskes, M.I., 2002. Interpretation of indentation size effects. J. Appl. Mech. 69, 433–442.
He, L.H., Lim, C.W., 2006. Surface Green function for a soft elastic half-space: influence of surface stress. Int. J. Solids Struct. 43, 132–143.
Huang, Y., Zhang, F., Hwang, K.C., Nix, W.D., Pharr, G.M., Feng, G., 2006. A model of size effects in nano-indentation. J. Mech. Phys. Solids 54, 1668–1686.
Huang, Z.P., Wang, J., 2006. A theory of hyperelasticity of multi-phase media with surface/interface energy effect. Acta Mech. 182, 195–210 (Erratum. Acta Mech. 215, pp. 365–366).
Huang, Z.P., Sun, L., 2007. Size-dependent effective properties of a heterogeneous material with interface energy effect: from finite deformation theory to infinitesimal strain analysis. Acta Mech. 190, 151–163 (Erratum. Acta Mech. 215, pp. 363–364).
Johnson, K.L., Kendall, K., Roberts, A.D., 1971. Surface energy and the contact of elastic solids. Proc. R. Soc. London A 324, 301–313.
Johnson, K.L., 1985. Contact Mechanics. Cambridge University Press, London.
Jing, G.Y., Duan, H.L., Sun, X.M., Zhang, Z.S., Xu, J., Li, Y.D., Wang, J.X., Yu, D.P., 2006. Surface effects on elastic properties of silver nanowires: contact atomic-force microscopy. Phys. Rev. B 73, 235409.
Koguchi, H., 2008. Surface Green function with surface stresses and surface elasticity using Stroh's formalism. J. Appl. Mech. 75, 061014.
Long, J.M., Wang, G.F., Feng, X.Q., Yu, S.W., 2012. Two-dimensional Hertzian contact problem with surface tension. Int. J. Solids Struct. 49, 1588–1594.
Ma, Q., Clarke, D.R., 1995. Size dependent hardness of silver single-crystals. J. Mater. Res. 10, 853–863.
Miller, R.E., Shenoy, V.B., 2000. Size-dependent elastic properties of nanosized structural elements. Nanotechnology 11, 139–147.
Medasani, B., Vasiliev, I., 2009. Computational study of the surface properties of aluminum nanoparticles. Surf. Sci. 603, 2042–2046.
Mohammadi, P., Sharma, P., 2012. Atomistic elucidation of the effect of surface roughness on curvature-dependent surface energy, surface stress and elasticity. Appl. Phys. Lett. 100, 133110.
Mohammadi, P., Liu, L.P., Sharma, P., Kukta, R.V., 2013. Surface energy, elasticity and the homogenization of rough surfaces. J. Mech. Phys. Solids 61, 325–340.
Nix, W.D., Gao, H., 1998. Indentation size effects in crystalline materials: a law for strain gradient plasticity. J. Mech. Phys. Solids 46, 411–425.
Park, H.S., Klein, P.A., 2008. Surface stress effects on the resonant properties of metal nanowires: the importance of finite deformation kinematics and the impact of the residual surface stress. J. Mech. Phys. Solids 56, 3144–3166.
Streitz, F.H., Cammarata, R.C., Sieradzki, K., 1994a. Surface-stress effects on elastic properties. I. Thin metal films. Phys. Rev. B 49, 10699–10706.
Streitz, F.H., Cammarata, R.C., Sieradzki, K., 1994b. Surface-stress effects on elastic properties. II. Metallic multilayers. Phys. Rev. B 49, 10707–10716.
Selvadurai, A.P.S., 2000. Partial Differential Equations in Mechanics, Vol. 2. Springer, New York.
Sharma, P., Ganti, S., Bhate, N., 2003. Effect of surfaces on the size-dependent elastic state of nano-inhomogeneities. Appl. Phys. Lett. 82, 535–537.
Sharma, P., Ganti, S., 2004. Size-dependent Eshelby's tensor for embedded nano-inclusions incorporating surface/interface energies. J. Appl. Mech. 71, 663–671.
Sharma, P., Wheeler, L.T., 2007. Size-dependent elastic state of ellipsoidal nano-inclusions incorporating surface/interface tension. J. Appl. Mech. 74, 447–454.
Wang, J., Duan, H.L., Huang, Z.P., Karihaloo, B.L., 2006. A scaling law for properties of nano-structured materials. Proc. R. Soc. A 462, 1355–1363.
Wang, G.F., Feng, X.Q., 2007. Effects of surface stresses on contact problems at nanoscale. J. Appl. Phys. 101, 013510.
Weissmuller, J., Duan, H.L., 2008. Cantilever bending with rough surfaces. Phys. Rev. Lett. 101, 146102.
Wang, Y., Weissmuller, J., Duan, H.L., 2010. Mechanics of corrugated surfaces. J. Mech. Phys. Solids 58, 1552–1566.
Zhao, X.J., Rajapakse, R.K.N.D., 2009. Analytical solutions for a surface-loaded isotropic elastic layer with surface energy effects. Int. J. Eng. Sci. 47, 1433–1444.
Zhao, Y.P., 2012. Some characteristic lengthscales, time scales and dimensionless numbers relevant to interfacial problems in nano- and micro-systems. In: Chen, J.K., Bai, S.L., Hu, G.K. (Eds.), Proceedings of national symposium on nonlinear behaviors of materials, Beijing, pp. 25–38. (in Chinese).